Radial bunch compression: Path-length compensation in an rf photoinjector with a curved cathode

M. J. de Loos, S. B. van der Geer, Y. M. Saveliev, V. M. Pavlov, A. J. W. Reitsma, S. M. Wiggins, J. Rodier, T. Garvey, D.A. Jaroszynski

Radial bunch compression: Path-length compensation in an rf photoinjector with a curved cathode

M. J. de Loos,[1,2,*] S. B. van der Geer,[1] Y. M. Saveliev,[2] V. M. Pavlov,[2] A. J. W. Reitsma,[2] S. M. Wiggins,[3,2] J. Rodier,[4] T. Garvey,[4] and D. A. Jaroszynski[2,†]

[1]*Pulsar Physics, Burghstraat 47, 5614 BC Eindhoven, The Netherlands*
[2]*SUPA, Department of Physics, University of Strathclyde, Glasgow G4 0NG, United Kingdom*
[3]*Department of Physics, Lancaster University, Bailrigg, Lancaster LA1 4YB, United Kingdom*
[4]*Laboratoire de l'Accélérateur Linéaire, Université de Paris-Sud, Centre Scientifique d'Orsay, IN2P3-CNRS, France*

(Received 9 June 2006; published 25 August 2006)

Electron bunch lengthening due to space-charge forces in state-of-the-art rf photoinjectors limits the minimum bunch length attainable to several hundreds of femtoseconds. Although this can be alleviated by increasing the transverse dimension of the electron bunch, a larger initial radius causes path-length differences in both the rf cavity and in downstream focusing elements. In this paper we show that a curved cathode virtually eliminates these undesired effects. Detailed numerical simulations confirm that significantly shorter bunches are produced by an rf photogun with a curved cathode compared to a flat cathode device. The proposed novel method will be used to provide 100 fs duration electron bunches for injection into a laser-driven plasma wakefield accelerator.

DOI: 10.1103/PhysRevSTAB.9.084201 PACS numbers: 29.27.Ac, 29.27.Bd, 41.75.Ht, 41.85.Lc

I. INTRODUCTION

Ultrashort high-brightness bunches of electrons with relativistic energies and durations of much less than 1 picosecond are required for numerous applications such as injection into accelerators or free-electron lasers (FELs) and for direct use in applications such as pulsed radiolysis [1] and time resolved electron diffraction [2]. These applications typically require electron bunches of a few MeV, with durations ideally of the order of a hundred femtoseconds or less. One application of ultrashort electron bunches with energies of several MeV is as an injector for the latest generation of laser-driven plasma wakefield accelerators [3].

This new technology imposes stringent requirements on the electron bunch duration, which should be less than 100 fs because of the short length scale of the acceleration ''structure'' due to traveling plasma waves, which have a wavelength of 100 μm or less. For the new technology to be useful, injected electron bunches should also have a relatively high charge, ideally in the range of 10–100 pC. Wakefield accelerators have the potential of revolutionizing x-ray radiation sources such as the free-electron laser by making them more compact and with shorter pulse duration, and could provide a new ''building block'' for the next generation of TeV colliders. Furthermore, a compact photoinjector is an ideal electron source for driving coherent spontaneous or superradiant free-electron lasers and transition radiation sources operating at terahertz frequencies because the bunch length is shorter than the emitted radiation wavelengths.

A method that seems ideally suited for the production of ultrashort electron bunches is the rf photoinjector [4]. In this device electron bunches with a charge up to several nC are photoextracted from a cathode surface that forms part of a resonant accelerating structure. Photoinjectors are efficient accelerators that produce high quality electron bunches. However, they have a major drawback in that the typical bunches produced by a single rf photoinjector structure have durations of the order of 1 or more picoseconds and are therefore too long for applications requiring ultrashort duration bunches, as mentioned above, even for charges as low as 10 pC.

A common method for producing ultrashort electron bunches in an accelerator is off-crest acceleration of a relatively long electron bunch (several picoseconds) and subsequent magnetic compression, as is done, for example, at the TTF at DESY [5]. However, compression is usually carried out at relatively high energies and using several accelerating structures and magnetic compression chicanes. For the applications mentioned above, the scheme is large, complex, and expensive.

An alternative approach to producing ultrashort duration bunches is by ballistic or velocity bunching of suitably phased electron bunches, see for example [6]. Here, an additional rf buncher induces a correlated velocity phase-space distribution such that the front of the bunch travels slower than the back. Compression occurs either ballistically at a longitudinal position at some point after the buncher or inside the buncher itself, in both cases resulting in short bunches with low emittance. Although the method works particularly well for ellipsoidal bunches [7] and can be incorporated in one single device [8],

*Electronic address: mloos@pulsar.nl
†Corresponding author.
Electronic address: dino@phys.strath.ac.uk

it always requires additional independently phased rf power.

This paper describes a novel concept for producing 100 fs duration electron bunches from a single rf photoinjector structure. In contrast to velocity bunching techniques, our method takes into consideration that electron beam focusing systems, such as solenoids and quadrupole magnets, are radially nonisochronous. This is because, unlike optical focussing elements, there is no additional phase delay accompanying the deflection of beamlets. We show that our method allows the beam diameter to be increased, thereby drastically reducing space-charge induced bunch lengthening. The additional path lengths of electrons distant from the axis can be compensated by either illuminating the photocathode using a curved phase-front ultrashort UV laser pulse, or by shaping the cathode with a curvature which introduces a radially dependent phase delay that precisely compensates the additional radially dependent path lengths. A very elegant feature of our proposed radial bunch compression scheme is that all cylindrically symmetric path-length differences downstream introduced by focusing elements can simultaneously be compensated.

Although the concept of a curved cathode is far from new and it is widely used because of its focusing properties, it has to our best knowledge never been proposed as a method of compensating downstream path-length differences to compress electron bunches to ultrashort durations.

II. SETUP

An important application of an ultrashort pulse photoinjector is as an injection source for a laser-driven wake field accelerator (LWFA). The project Advanced Laser Plasma High-energy Accelerators towards X-rays (ALPHA-X) aims to develop a laser-driven wakefield accelerator and apply it to the creation of a compact free-electron laser (FEL) [3,9,10]. Wakefield accelerators are predicted to produce sub-ten-femtosecond electron bunches with energies as high as several GeV with gradients 3 orders of magnitude higher than those available from conventional accelerators [11]. To achieve the goal of developing a laser-driven accelerator and utilize it to drive a coherent radiation source, a number of significant challenges need to be met. Several techniques for injecting ultrashort electron bunches into a plasma channel [12], which acts as the extended accelerating medium, need be investigated. Two different injection approaches are being investigated as part of the Alpha-X project. The first of these is a compact all optical method, which involves extracting electrons directly from the background plasma using an intense ultrashort laser pulse and injecting it into the wakefield accelerator [13]. In parallel to these investigations, an S-band 6 MeV photoinjector has been developed to externally inject suitable ultrashort bunches, with durations of the order of the plasma-wake period, which will allow concepts of staging, bunching, and scaling to be investigated for future TeV accelerator stages.

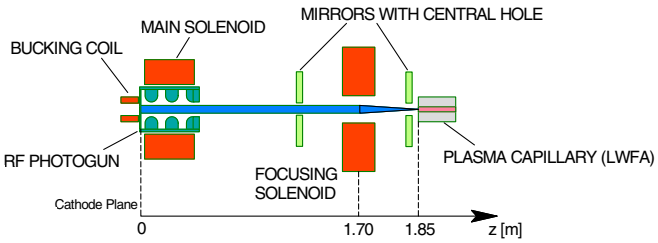

FIG. 1. (Color) Schematic of the Alpha-X setup.

Alpha-X aims at injected bunches with a duration of 100 fs and with an emittance small enough, 1–4 μm, to allow the electron bunch to be focused to a spot size of approximately 35 μm, sufficiently small to match the plasma-wake dimensions [3,12]. Figure 1 shows schematically the Alpha-X injector beam line, which also includes the plasma accelerator at the final focus. The front end of the beam line consists of a 2.5 cell S-band rf photoinjector with an axial rf input coupler, similar to the one described in [14]. The cavity sustains a maximum field on axis of 100 MV/m which is used to accelerate electrons to 6.25 MeV. Elliptically shaped irises reduce the field on the iris surface below that of the cathode field. A solenoid with a nominal field of 0.25 T is used to produce a parallel beam. An additional focusing solenoid of about 0.5 T further downstream focuses the beam sharply to a spot size below 50 μm onto the entrance of a plasma capillary. A mirror with a small aperture is used to focus the high-power (20 TW) laser onto the entrance of the capillary to excite the accelerating plasma wave.

III. SIMULATION MODEL

The setup presented in the previous section has been designed with the general particle tracer (GPT) code [15,16]. This software package calculates the trajectories of up to a million sample particles in 3D, through the combined external and space-charge fields. A 5th order embedded Runge-Kutta solver [17] is used to integrate the relativistic equations of motion in the time domain. The integration steps are automatically chosen, based on a maximum tolerance of typically 10^{-5} for the dimensionless momentum coordinates, and span 6 orders of magnitude: a few fs in the cathode region, to the ps range in the last two cells of the cavity and towards the entrance of the plasma channel, to over 1 ns in the drift space between the two solenoids.

The cavity dimensions have been determined using the Superfish set of codes [18] and fed into GPT as high-precision field maps. We use identical spacing in the longitudinal and transverse direction of 10 μm in the cathode region, and relax this to 250 μm in the remainder of the device. The less-critical magnetostatic fields for the

bucking coil and focusing solenoids are imported into GPT on a much courser mesh of 1 by 1 mm. We observed that off-axis cavity fields calculated by first order Taylor expansion of the on-axis standing-wave electric field profile do not produce correct simulation results on femtosecond time scales. Experimentally however, the on-axis field has been used to cross-check the final dimensions against the Superfish results with a bead-pull measurement with excellent agreement and an overall field imbalance of only 1%.

Space-charge fields are calculated with a particle in cell (PIC) method, where Poisson's equation is solved in the rest frame of the bunch. Although the initial conditions, the cavity fields, and the solenoids are all cylindrically symmetric, space-charge forces still need to be calculated in 3D to obtain tolerances on misalignment and the effect of nonuniform emission from the cathode. This is challenging for high aspect-ratio bunches, and numerical instabilities are overcome with a tailor made 3D anisotropic multigrid Poisson solver with adaptive meshing based on bunch charge density, as described in detail in [19]. The effect of image charges can be included for a flat cathode, but not in the curved cathode case due to limitations of the multigrid space-charge model. It has been numerically verified that image charges do not play a significant role for the flat cathode case, and it is therefore assumed that they will not play a role in the curved cathode case either.

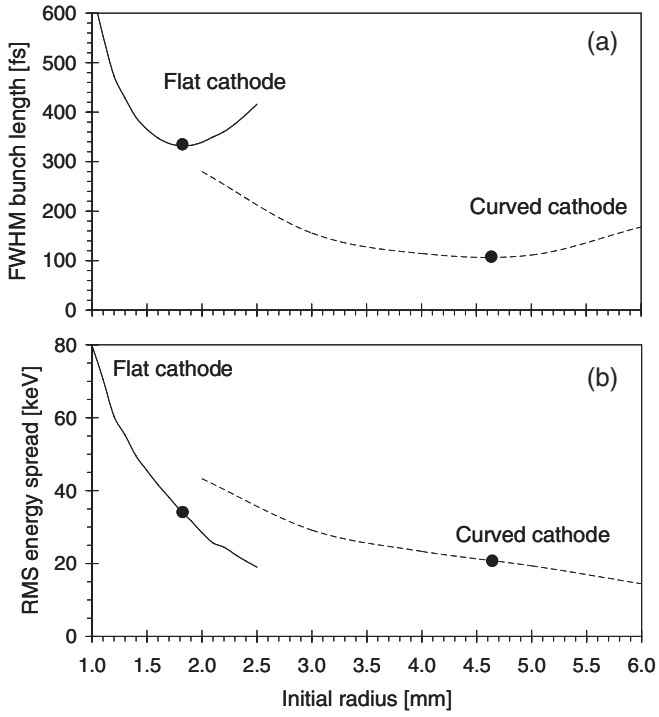

FIG. 2. (a) Bunch length of a 10 pC electron bunch at the entrance of the plasma channel at, $z = 1.85$ mm, as function of initial radius. (b) Corresponding energy spread. The initial radii resulting in minimum bunch lengths are indicated by dots.

IV. PATH-LENGTH DIFFERENCES

The currently accepted approach for producing short electron bunches from a single S-band photoinjector is to use an ultrashort duration, 30–50 fs, UV photoexcitation laser to illuminate typically a 1 mm radius surface area of the photocathode. In this so-called "pancake" regime, the asymptotic bunch length due to space-charge forces of a uniformly accelerated bunch, ignoring the initial laser-duration, assuming prompt response from the copper surface and under the conditions that the radius is kept constant, is given by [20]

$$\Delta t_{\mathrm{sc}}(\infty) = \frac{mc^2}{e}\frac{\sigma}{\epsilon_0 c E^2}. \tag{1}$$

Here $\sigma = Q/(\pi R^2)$ is the surface charge density of the bunch, Q and R are the bunch charge and radius, respectively, mc^2/e is the electron rest energy of 0.511 MeV, c is the speed of light, ϵ_0 is the permittivity of vacuum and E is the effective (average) acceleration field. If we assume a typical effective $E = 50$ MV/m for an S-band rf photogun, a total charge as low as 10 pC, with $R = 1$ mm, already results in an unacceptably long asymptotic bunch length of about 250 fs. The only free parameter is the initial radius, where the final bunch length scales with the inverse of the initial radius squared. An increase from 1 to 3 mm therefore reduces, in theory, the final bunch length to 30 fs, the same order as the duration of the photoexcitation pulse. However, as shown in Fig. 2(a), an increase in initial bunch radius is only partially effective for a flat cathode. The predicted significant decrease in bunch length with radius is clearly visible, but after 1.8 mm the bunch length starts to increase again.

To illustrate the mechanism that causes additional bunch lengthening at large radii, beam envelopes in the Alpha-X beam line are shown in Fig. 3(a) for an initial bunch radius of 1, 2, and 3 mm using the model described in the previous section. Figure 3(b) shows a "time-radius" radial phase-space snapshot of a 10 pC bunch as it passes a virtual screen located 1 m from the cathode. Particles are energy color coded to visualize the energy spread. The 1 mm initial radius bunch produced by the 30 fs photoexcitation laser is stretched to $\approx$ 400 fs by the space-charge induced energy dispersion. A 3 mm initial radius beam is much less sensitive to space-charge forces because of the lower charge density and therefore has a lower energy spread. However, the 3 mm radius bunch is about as long because it stretches due to the longer path lengths of the outer particles compared with electrons closer to the axis. This geometrically induced path-length dispersion always becomes the dominant effect at large initial radii because it scales with R^2, compared with R^{-2} for space-charge effects:

$$\Delta t_{\mathrm{path\ length}} = \alpha_2 R^2 + \alpha_4 R^4 + O(R^6). \tag{2}$$

In the case of the Alpha-X photoinjector, we numerically obtained the value for α_2 for the combined effect of rf

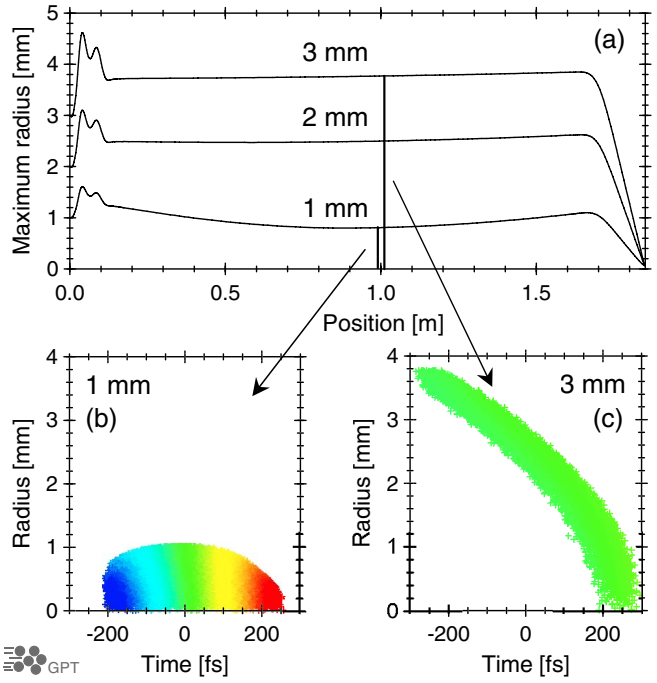

FIG. 3. (Color) (a) Typical beam envelopes in the Alpha-X beam line for various initial radii with a flat cathode. (b),(c) Simulated time-radius projection of the bunch at 1 m from the cathode plane, for 1 and 3 mm initial radius, respectively. The energy distribution is color coded with red: high energy and blue: low energy.

(de)focusing in the cavity and the solenoid. The resulting value of $\alpha_2(z = 1\ \mathrm{m}) = 52\ \mathrm{fs\,mm^{-2}}$ sets a maximum radius of 1.5 mm for a flat cathode before geometrical path-length differences cause bunch lengthening on the order of 100 fs. This coincides with the theoretical optimal initial bunch radius, close to the value of 1.8 mm found numerically.

Not mentioned thus far is geometric bunch lengthening due to downstream focusing elements. The term scales with R^2 and is given by

$$\Delta t_{\mathrm{geom}} \approx \frac{R^2}{fv} \tag{3}$$

with v the particle velocity. For the planned Alpha-X focusing distance of $f = 150$ mm into the plasma capillary, this effect of 20 fs $\mathrm{mm^{-2}}$ is smaller than the combined effect of the cavity and solenoid, but not sufficiently small that it can be ignored.

V. CURVED CATHODE

From the above discussion, it is clear that the final bunch length obtained with a single rf photogun and a flat cathode is set by a compromise between space-charge effects at small initial radius and path-length differences at large initial radius. Path-length differences however are not a fundamental limitation and in this section we show that they can be fully compensated for. This in turn allows us to shift the compromise to much larger initial radii, hereby significantly reducing space-charge effects. The same argumentation is valid for electrostatic accelerators as well.

To compensate path-length differences, we propose to predisperse the electron bunch in radial phase space. This can be achieved either by altering the laser wave front shape or by altering the cathode shape. The former is difficult to achieve with front illuminated cathodes because the focal length required to achieve the necessary wave front curvature on the cathode is very short, typically a few centimeters. This requires beam diameters, which are much larger than the typical iris dimensions. A back illuminated cathode is technically challenging given the high accelerating fields, which could exceed 100 MV/m. The easiest geometric dispersion compensation scheme is therefore to alter the cathode shape and use a plane wave to illuminate the cathode. It is possible to combine the curved cathode with a slightly curved laser wave front to fine-tune the compensation without remachining the cathode plane.

In the case of a curved cathode and a flat laser front, we see that there are two contributions to the axial/radial distributions that result in predispersed off-axis particles. First, outer particles have less distance to travel because they are born closer to the target. Second, they are photoextracted before the inner ones because the flat laser front arrives at the outer edge first. The combined effect is given by

$$\Delta t_{\mathrm{cc}} = (R_c - \sqrt{R_c^2 - R^2})\left(\frac{1}{c} + \frac{1}{v_{\mathrm{final}}}\right), \tag{4}$$

where R_c is the radius of curvature, R the bunch radius, c the speed of light, and v_{final} the final electron velocity. For relativistic particles and $R \ll R_c$ this reduces to

$$\Delta t_{\mathrm{cc}} = \frac{R^2}{cR_c}. \tag{5}$$

A rough estimate for the optimal radius of curvature is based on making the total R^2 dependency of the path-length differences equal to the R^2 term of the predispersion given by the curved cathode. In our case, this yields

$$\frac{1}{cR_c} = \alpha_2 + \frac{1}{fc} \tag{6}$$

resulting in an approximate value for the optimal curvature radius of 45 mm. This is relatively far off the numerically obtained ideal curvature radius of 80 ± 5 mm. The discrepancy is mainly caused by the fact that the transverse component of the rf field near the curved cathode has a well-known focusing effect. This in turn affects the trajectories by reducing space-charge expansion near the cathode and thereby reducing the path-length differences. Furthermore, the curvature locally reduces the longitudinal acceleration field on axis and as a result on-axis particles are initially accelerated less, resulting in a later arrival

time. Both effects combined increase the optimal curvature radius from 45 to 80 mm.

The dramatic improvement possible with a curved cathode is illustrated in Fig. 2(a). The plot shows the final bunch length for a curved cathode with optimal radius of curvature as function of initial bunch radius. The optimal initial bunch radius is shifted from 1.8 mm for the flat cathode case to 4.6 mm, reducing space-charge forces by more than a factor 6, and reducing the final bunch length from 330 fs to less than 100 fs FWHM. The bunch-length evolution corresponding to the optimal initial bunch radius for a flat cathode and for the curved cathode case are shown in Fig. 4a. The length of the bunch emitted from a flat cathode rises monotonically due to space-charge forces and path-length differences. This is in sharp contrast to the bunch emitted from a curved cathode that starts elongated, due to phase delays on axis, but reduces stepwise in length at each focusing element in the beam line to well below the value obtained with a flat cathode.

Figures 4(b) and 4(c) show the time-radius projections at the entrance of the plasma channel for the flat and curved cathode cases. Clearly, the curved cathode not only reduces the pulse duration, it also has a beneficial effect on spot size. This is mainly because a flat cathode introduces undesired mixing between different slices of the bunch: Off-axis particles arrive at the same longitudinal position as on-axis particles started later. This results in projected rms emittance growth, leading to a larger spot size. To prevent this mixing, and the accompanying emittance growth, slices need to be curved such that particles in one slice remain in this slice throughout the beam line. The rms spot size at the entrance of the plasma capillary is given by $\epsilon f/(\gamma R)$, where ϵ is the normalized rms emittance, f the focal distance of the solenoid, and γ the Lorentz factor. If we are able to maintain the initial thermal emittance, scaling linearly with approximately 0.5 μm per mm initial bunch radius, the ratio ϵ/R is constant resulting in a constant spot-size independent of the initial bunch radius. As shown in Fig. 5, this is achieved with a curved cathode for initial radii as large as 3.5 mm, which is the radius where higher order effects slowly begin to play a role. This is in sharp contrast with the flat cathode case, where the emittance deviates strongly from the initial thermal emittance due to mixing, resulting in a larger spot size for all relevant initial radii. Additional beneficial effects of a curved cathode on the transverse dynamics are that a larger initial radius reduces space-charge induced emittance growth. Furthermore, a curved cathode reduces space-charge induced energy spread, which in turn makes the spot-size less sensitive to the chromatic aberrations of the focusing system. Finally, the focusing properties of a curved cathode relax the need for a focusing solenoid and aid the emittance compensation process, see [21] describing the beneficial effects of initial radial focusing in a similar structure.

At very large initial radii, a spherical dimple will not be the ideal shape. This leads to a natural extension of the presented concept to higher-order correction, where an

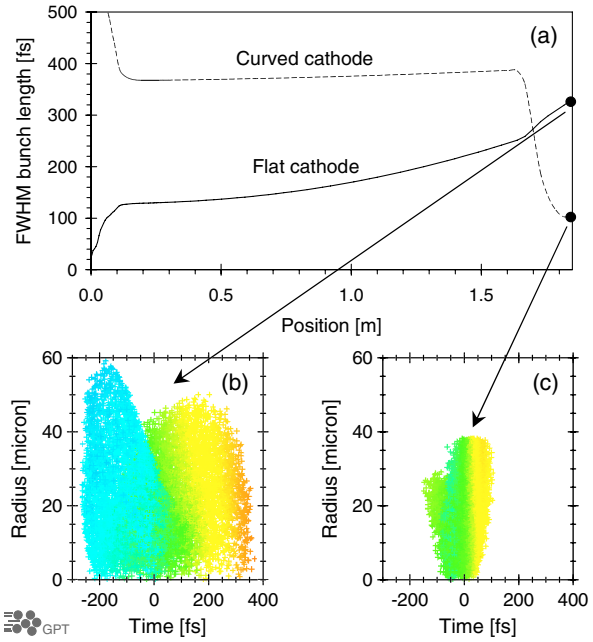

FIG. 4. (Color) (a) Bunch-length evolution of a 10 pC electron for a flat and curved cathode. (b),(c) Simulated time-radius projection at the entrance of the plasma channel. (b) Flat cathode case. (c) Curved cathode with 80 mm radius. Particles are color coded on energy with the same scale as Fig. 3.

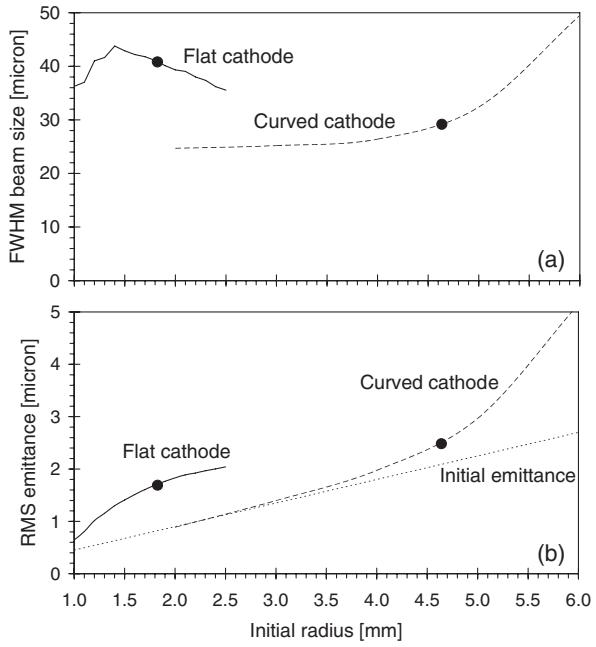

FIG. 5. (a) FWHM spot size at the entrance of the plasma channel as a function of initial radius for a 10 pC bunch. (b) Corresponding emittance. The dashed line indicates the initial thermal emittance. The initial radius resulting in minimum bunch length is indicated by the dots.

elliptically shaped curvature is the next shape to consider. This refinement will shift the minimum bunch length toward larger initial radii and result in even shorter bunches. However, accommodating a bunch with ever larger radius may be difficult because of beam transport line constraints, e.g. in the case of Alpha-X the first constraint is the radius of an aperture in the mirror focusing the high-power laser into the plasma channel to drive the plasma wake. Furthermore, the antenna of the axial incoupling and the irises of the rf photogun itself set well-defined limits on the maximum allowed bunch radius.

A larger initial radius also results in larger initial thermal emittance. At some point this will be unacceptable for the application of the produced bunches, for example, because the bunch cannot be focused tightly on the target anymore. There are no technical solutions for this problem, because femtosecond lasers are broadband, leading to excess energy in the photoemission process that in turn results in an initial thermal emittance that scales linearly with the initial radius of the bunch. The larger initial thermal emittance is therefore a fundamental limiting factor of the applicability of a curved cathode, where it should be noted that for small initial radii a curved cathode improves the final rms emittance.

Although it makes perfect sense to increase the initial bunch radius with a curved cathode to accommodate more charge, there is no point in trying to reduce the final pulse duration to below a few times ten femtoseconds. At that time scale processes other than space charge, such as the finite duration of the excitation laser, the response time of copper, and thermal energy spread due to broadband femtosecond photoionization, set the minimal achievable bunch length.

VI. EXPERIMENTAL REALIZATION

Figure 6 shows a schematic giving the cavity dimensions. Superfish simulations were used to predict the gun dimensions needed to obtain the required π mode frequency (2998.55 MHz) of the $2\frac{1}{2}$ cell standing-wave structure. The curved cathode has a small dimple at the center to compensate for the path-length differences, as shown on a 5:1 scale in detail A. A compensation groove is machined close to the outer edge, see detail B, to allow the curved backplate to be replaced with a flat cathode without changing the resonance frequency or field balance.

The rf gun and its input coupler have been constructed "in house" by the Laboratoire de l'Accélérateur Linéaire, d'Orsay. The cavity cells are machined on a numerical controlled lathe using a single-point diamond tool. As the available machining accuracy is limited to $\sim$20 μm, the initial cell diameters are machined to be smaller (by $\sim$100 μm) than the calculated values so that the desired resonance frequency could be approached in an iterative fashion. Low power measurements of the cavity frequency between successive machining operations, and the frequency sensitivity to cell radius (given by Superfish simulations), enabled an estimate of the amount of material to remove on each iteration. The low power measurements are made at ambient pressure, whereas the gun operates under vacuum. This results in a calculable shift in the mode frequency ($\sim$ 900 kHz) which must be allowed for. However, the brazing of the cells produces an additional frequency shift for which the value, in general, is difficult to predict. Previous experience shows that this increases the resonant frequency (the increase finally observed was 220 kHz). Therefore, we initially aimed for a lower value

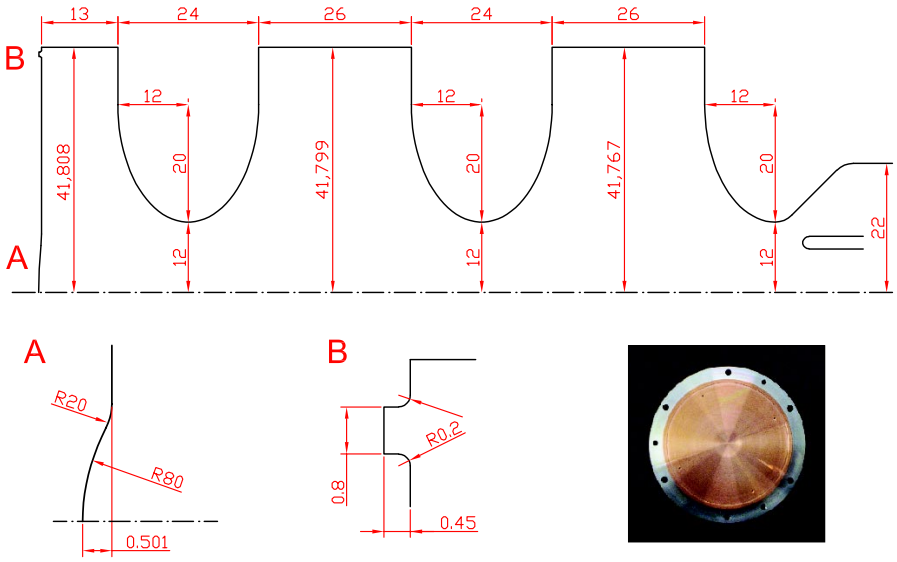

FIG. 6. (Color) Simplified inner dimensions of the rf-photogun with curved cathode. Detail A shows the dimple to compensate for path-length differences on a 5:1 aspect ratio, detail B shows the compensation groove with 1:1 aspect ratio.

(~ 2998.15 MHz) knowing that fine-tuning of the operating frequency could be achieved by regulating the operating temperature around the intended nominal value of 30 °C via the cooling system (~ -50 kHz/ deg) or by dimple tuning, i.e., by a slight deformation of the cell diameter at discrete points. The rf gun to klystron connection is made through a ''doorknob'' type waveguide to coaxial transition coupler. Radio-frequency tests of the coupler required the use of special, custom built, conical coaxial adapters to match the 50 Ω antenna to a standard $\frac{7}{16}$ inch connecter. The use of the conical adapter allows the short circuit position of the input waveguide to be optimized, yielding a -40 dB return loss of the coupler into a matched load.

The input antenna was initially machined to be over coupled to the cavity. Matching it to the cavity was performed by gradually reducing the antenna length to obtain a voltage standing-wave ratio (VSWR) ~ 1.03. The final position of the antenna tip with respect to the iris of the cavity output cell was within 0.1 mm of the value predicted by rf simulations. In order to be demountable, the cathode is brazed to a stainless steel flange which can be screwed onto a flange on the $\frac{1}{2}$ cell of the gun. The cathode was electropolished to produce a ''mirrorlike'' surface with the aim of reducing the dark current level. The final rf measurements, after brazing of the gun cells and the input coupler, gave a resonant frequency of 2998.24 MHz at a temperature of 20 °C and a pressure of 760 mbar. To obtain the required frequency under vacuum implies that the gun must be operated at 32 °C. The measured quality factor of the cavity after brazing was 10 900 and the overall VSWR of the cavity equipped with its coupler was equal to 1.04. Bead-pull perturbation measurements of the cavity show that the peak electric field in the three cells is well balanced, with less than 3% difference from cell to cell.

VII. CONCLUSION AND DISCUSSION

A curved cathode can be used to predisperse an electron bunch to compensate downstream path-length differences in both rf and electrostatic accelerators. The combination of curved cathode and focusing systems acts as an effective radial bunch compressor. The relaxed constraint on initial bunch radius allows a significant reduction in space-charge induced bunch lengthening. In addition, the final rms emittance is lowered to near the initial thermal emittance. In the case of the Alpha-X experiment, a curved cathode reduces the bunch length from over 300 to 100 fs for a 10 pC bunch. There are no restrictions on the use of a curved cathode regarding downstream applications, as long as the final emittance is tolerable. A curved cathode is therefore fully compatible with ballistic and velocity bunching to compensate path-length differences. Because the concept sets no restrictions on the initial transverse charge distribution, it is expected to be beneficial for the creation and compression of ellipsoidal bunches as well.

ACKNOWLEDGMENTS

We gratefully acknowledge financial support from the Research Councils UK Basic Technology Programme.

[1] Y. Muroya, T. Watanabe, G. Wu, X. Li, T. Kobayashi, J. Sugahara, T. Ueda, K. Yoshii, M. Uesaka, and Y. Katsumura, Radiat. Phys. Chem. **60**, 307 (2001).
[2] B. J. Siwick, J. R. Dwyer, R. E. Jordan, and R. J. D. Miller, Science **302**, 1382 (2003).
[3] D. A. Jaroszynksi *et al.*, Phil. Trans. R. Soc. A **364**, 689 (2006).
[4] K. T. McDonald, IEEE Trans. Electron Devices **35**, 2052 (1988).
[5] DESY-TTF, Hamburg, Germany, http://tesla.desy.de
[6] S. G. Anderson *et al.*, Phys. Rev. ST Accel. Beams **8**, 014401 (2005).
[7] S. B. van der Geer *et al.*, Phys. Rev. ST Accel. Beams **9**, 044203 (2006).
[8] J. W. Lewellen, Proceedings of the 2003 Particle Accelerator Conference (2003), p. 2035.
[9] http://phys.strath.ac.uk/alpha-x/index.html
[10] D. A. Jaroszynki and G. Vieux, *Advanced Accelerator Concepts*, AIP Conf. Proc. No. 647 (AIP, New York, 2002), pp. 902–913.
[11] E. Esarey, P. Sprangle, J. Krall, and A. Ting, IEEE Trans. Plasma Sci. **24**, 252 (1996).
[12] A. Butler, D. J. Spence, and S. M. Hooker, Phys. Rev. Lett. **89**, 185003 (2002).
[13] Th. Katsouleas, Nature (London) **431**, 515 (2004); S. P. D. Mangles *et al.*, Nature (London) **431**, 535 (2004); C. G. R. Geddes *et al.*, Nature (London) **431**, 538 (2004); J. Faure *et al.*, Nature (London) **431**, 541 (2004).
[14] F. B. Kiewiet, Ph.D. thesis, Eindhoven University of Technology, 2003.
[15] http://www.pulsar.nl/gpt
[16] S. B. van der Geer, O. J. Luiten, M. J. de Loos, G. Pöplau, and U. van Rienen, *3D Space-Charge Model for GPT Simulations of High Brightness Electron Bunches*, Institute of Physics Conference Series No. 175 (Institute of Physics, Bristol, UK, 2005), p. 101.
[17] W. H. Press *et al.*, *Numerical Recipes, The Art of Scientific Computing* (Cambridge University Press, Cambridge, England, 1992), 2nd ed.
[18] J. H. Billen and L. M. Young, Los Alamos National Laboratory, Report No. LA-UR-96-1834.
[19] G. Pöplau, U. van Rienen, S. B. van der Geer, and M. J. de Loos, IEEE Trans. Magn. **40**, 714 (2004).
[20] O. J. Luiten, in *The Physics and Applications of High Brightness Electron Beams*, edited by J. Rosenzweig, G. Travish, and L. Serafini (World Scientific, Singapore, 2003), p. 108.
[21] D. Janssen and V. Volkov, Nucl. Instrum. Methods Phys. Res., Sect. A **452**, 34 (2000).